

ORIGINAL ARTICLE

Application of benzonase in preparation of decellularized lamellar porcine corneal stroma for lamellar keratoplasty

Jing Liu¹ | Zhihan Li¹ | Jie Li¹ | Zuguo Liu^{1,2,3} 

¹Fujian Provincial Key Laboratory of Ophthalmology and Visual Science, Eye Institute of Xiamen University; College of Medicine, Xiamen University, Xiamen, Fujian Province, China

²Xiang'an Hospital of Xiamen University

³Xiamen Eye Center of Xiamen University

Correspondence

Zuguo Liu, Fujian Provincial Key Laboratory of Ophthalmology and Visual Science, Eye Institute of Xiamen University, College of Medicine, Xiamen University, 4th Floor, Chengyi Building, Xiang'an campus of Xiamen University, Xiang'an South Road, Xiamen 361001, Fujian Province, China.
Email: zuguoliu@xmu.edu.cn

Funding information

National Key R&D program of China, Grant/Award Number: 2018YFA0107304

Abstract

This study was to develop a novel and efficient method using endonuclease (benzonase) to prepare decellularized lamellar porcine corneal stroma (DLPCS). The DLPCS was prepared from native lamellar porcine corneal stroma (NLPCS) and was treated with 1000 U/ml benzonase for 5 hours. We conducted the following measurements and animal transplantation to compare DLPCS and NLPCS. The residual DNA was decreased significantly from 367.13 ± 19.96 ng/mg to 15.41 ± 0.65 ng/mg after treatment of benzonase by the detection of fluorescent nucleic acid stain. The residual benzonase was also less than detection limit. There was no significant difference in light transmittance of DLPCS compared with NLPCS. The extracts of DLPCS did not inhibit cell proliferation of human corneal epithelial cells, mouse fibroblast (L-929) and African green monkey kidney cell (Vero cell). The DLPCS was transplanted into the corneas of rabbit by lamellar keratoplasty. There was no corneal melting and graft rejection observed within 12 months. The images demonstrated that the repairment of corneal nerves and keratocytes of DLPCS were in identical shape and reflection compared with normal cornea, and no obvious inflammatory cells were observed postoperation, by *in vivo* confocal microscopy. We provided novel evidence that the application of benzonase may improve the quality of DLPCS.

KEYWORDS

benzonase, bioengineered cornea, decellularized cornea, keratoplasty

1 | INTRODUCTION

Porcine corneal stroma is a possible suitable substitute for human corneal donor tissue in lamellar keratoplasty, which involves selective removal and replacement of diseased opaque corneal layers and has a much lower rejection risk than penetrating keratoplasty in allogeneic corneal transplantation (Akanda et al., 2015). Because of the lack of cornea donors in Asian countries, many patients with stromal opacification may suffer from stromal dystrophy, infection, inflammation, or trauma and may lose the ability to recover their vision after the first attempt at lamellar keratoplasty (Ekser et al., 2012). Decellularized mammal

corneas have better ultrastructure and biocompatibility than fabricated artificial corneas (Lai & Tang, 2014). Decellularized porcine corneal stroma is considered the best source for human lamellar corneal transplantation due to its stromal thickness, similar extracellular matrix (ECM) components and collagen arrangement (Lee et al., 2017). Moreover, our previous study found that its corneal anterior curvature and thickness are similar to those in humans and most mammals, except for primates.

Porcine corneal stroma, which is identical to human corneal stroma, has a highly organized arrangement (Bueno, Gualda, & Artal, 2011). Experimental evidence has indicated that porcine corneas are

This is an open access article under the terms of the Creative Commons Attribution-NonCommercial-NoDerivs License, which permits use and distribution in any medium, provided the original work is properly cited, the use is non-commercial and no modifications or adaptations are made.

© 2019 The Authors. *Journal of Biomedical Materials Research Part A* published by Wiley Periodicals, Inc.

sufficiently similar to human corneas in terms of biomechanical parameters, suggesting that porcine cornea is likely to provide a successful alternative to human keratoplasty (Hara & Cooper, 2011). There are several decellularization techniques that have been used in dozens of decellularized mammal tissues throughout Europe and the United States, the most commonly used agents for decellularization are detergents (Crapo, Gilbert, & Badylak, 2011). However, damage to porcine corneal collagen fibrils by detergents is notable. Decellularization destroys the microstructure of collagen fibrils and disturbed corneal fibril arrangement and spaces lead to corneal opacification by increasing the amount of refracted, scattered, and reflected light (Y1, Wong, Monson, Stringham, & Ambati, 2010). Moreover, high level of reagents remained from decellularization process has a risk of corneal inflammation and influences corneal stromal cells reconstruction after lamellar keratoplasty. Stromal keratocytes are scattered among collagen fibril lamellae, remain relatively quiescent in normal corneas, and are stimulated in environments containing injured or inflamed stroma. After the application of detergents for decellularization, porcine corneal stroma becomes opaque and does not completely recover within 6 months postlamellar keratoplasty, and three cases have shown corneal melting symptoms (Zhang et al., 2015).

Porcine DNA and cellular proteins, including soluble and insoluble proteins, are two major targets for decellularization processes. We aimed to develop a gentle decellularization process with minimal damage to collagen fibrils and proteoglycan. Therefore, we investigated the degradation of soluble proteins and DNA, which are difficult to degrade using detergents. In the present study, we used benzonase, which is a genetically engineered endonuclease that digests DNA and RNA into 5'-monophosphate-terminated oligonucleotides that are 3 to 5 bases in length, as a decellularizing enzyme. The nucleotide fragments and soluble proteins can be dissolved from corneal stroma without substantially damaging collagen fibrils. Benzonase has been used in vaccine preparation to remove genetically bioengineered nucleotides and decellularize the dermis (Bertasi, Cole, Samsell, Qin, & Moore, 2017; Fischer, Wolff, & Reichl, 2018; Moore et al., 2015). In this study, we investigated the decellularization of porcine corneal stroma by using benzonase to prepare corneal tissue engineering scaffolds for human lamellar keratoplasty and improve the procedure for the decellularization of porcine corneal stroma.

2 | MATERIALS AND METHODS

2.1 | Animals

Whole porcine eyes (Wuzhishan, 5–7 month male and female pigs weighing 50–70 kg) were obtained from Yunnan Agricultural University within 1–2 hr postmortem and subjected to a decellularization procedure within 1 hr after obtaining the eyes. The eyes that were used in this study had an integral corneal surface with a horizontal corneal diameter of 12–14 mm and an initial corneal thickness of 650–850 μm , as indicated by a corneal pachymeter (TOMEY, Japan). The native lamellar porcine cornea stroma (NLPCS) was drilled by

10 mm trephination, and the epithelium and endothelium were removed by mechanical force. Male and female New Zealand white rabbits aged 10 weeks and weighing 2–4 kg were used as animal transplant models for lamellar keratoplasty. The animal experiments were carefully performed in accordance with the ARVO Statement for the Use of Animals in Ophthalmic and Vision Research, and the animal experimental protocol was approved by the Animal Ethics Committee of the Medical College of Xiamen University.

2.2 | Preparation of decellularization solution

Decellularization solution I consisted of 120 mM NaCl, 5.5 mM KCl, 1.2 mM CaCl_2 , 0.8 mM MgSO_4 , and 30 mM NaHCO_3 (pH 7.5, 310 mosmol/kg). Decellularization solution II contained antibiotics (100 IU/mL penicillin, 100 mg/mL streptomycin, and 0.625 mg/mL amphotericin). Decellularization solution III consisted of decellularization solution I and benzonase (1000 U/mL; Merck, Germany). Antibiotics were added to all the solutions, and the solutions were sterilized through a 0.22 μm pore filter.

2.3 | Decellularization procedures

Each NLPCS was weighed to obtain an initial weight. After washing three times for 20 min per wash in decellularization solution II, the samples were immersed in decellularization solution III for 5 hr at 25°C followed by washing 6 times for 30 min per wash in PBS at 25°C to remove residual benzonase and soluble proteins. All steps were conducted with continuous shaking in a water bath at a controlled temperature. To prepare decellularized lamellar porcine corneal stroma (DLPCS), NLPCS was sealed in a sterile plastic envelope, sterilized by γ -irradiation (20 kGy), and stored at 4°C before use.

2.4 | Histology and immunohistochemistry

NLPCS and DLPCS ($n = 3$ in each group) were embedded in O.C.T. compound (Tissue Freezing Medium) and cut into 5-mm-thick sections. Then, the sections were stained with hematoxylin and eosin (H&E) and examined under a light microscope (Carl Zeiss, Germany).

2.5 | Residual DNA analysis

Whole NLPCS and DLPCS ($n = 5$ per assay) were dried to a constant weight in a cabinet drier at 37°C for 72 hr and weighed until a stable weight was achieved. The samples were digested with 125 mg/mL proteinase K (Sigma) at 37°C for 24 hr. Whole DNA was extracted from each sample by phenol-chloroform (Sigma). The residual DNA in DLPCS and NLPCS was quantified by a Quant-iT PicoGreen Assay (Invitrogen, Germany) according to the manufacturer's instructions.

2.6 | Electron microscopy for ultrastructural analysis

NLPCS and DLPCS ($n = 3$ in each group) were fixed with 2.5% glutaraldehyde in phosphate buffer (pH 7.0) for 6 hr, postfixed with

1% OsO₄ in phosphate buffer (pH 7.0) for 1 hr, dehydrated in a graded series of ethanol (30, 50, 70, 80, 90, 95, and 100%) for 20 min for each concentration, transferred to absolute acetone for 20 min, placed in capsules containing embedding medium and heated at 70°C for approximately 9 hr. All the specimen sections were stained by uranyl acetate and alkaline lead citrate for 15 min and observed by transmission electron microscopy (TEM) using a model of H-7650.

2.7 | Assay for residual benzonase

After the dry weight was obtained, each DLPCS was soaked in 1 mL PBS at 37°C for 24 hr. The residual benzonase endonuclease in leaching liquor was analyzed by benzonase ELISA Kit II (Merck).

2.8 | Light transmittance assay

NLPCS and DLPCS samples were placed in glycerol (Invitrogen) for 2 hr before light transmittance evaluation. The spectral transmittance was measured at a wavelength of 380–780 nm using a Shimadzu UV-3600 spectrophotometer (Japan) and glycerol as a blank control. The transmittance was measured in 10 nm steps. The transmission coefficient (C_t) was calculated using the following equation: $C_t = I_t/I_0$, where I_t is the intensity of transmitted light, and I_0 is the intensity of incident light. Each sample was analyzed three times.

2.9 | Extract cytotoxicity assay

Each DLPCS (10 mm diameter) was extracted at 37°C for 24 hr in 1 mL normal medium (DMEM supplemented with 15% heat inactivated fetal bovine serum, Gibco BRL) to prepare leaching liquid. Human corneal epithelial cells (1×10^3 cells) were seeded into each well of 96-well plates and cultured with experimental (DLPCS leaching liquid, $n = 10$), positive control (DMSO, $n = 10$) and negative control (DMEM, $n = 10$) groups. After 1, 3, 5, and 7 days, the proliferation of the cells was quantitatively analyzed by an MTS assay (Promega). The optical density (OD) of the absorbance at a wavelength of 490 nm was measured by a microplate reader.

2.10 | Lamellar keratoplasty in rabbits

Twelve DLPCSs (100 mm and 6.50 mm diameter) were implanted into the right eyes (DLPCS-transplanted group) of 12 rabbits by lamellar keratoplasty. Contralateral corneas that did not undergo an operation served as the control group. Briefly, for lamellar keratoplasty, under general anesthesia, a 100 to 150-mm-deep and 6.25-mm-diameter circular incision was made using a trephine. Lamellar dissection was then performed using a scalpel along the natural uniform stratum in the corneal stroma to remove the host epithelium and anterior stroma. The DLPCS graft was sutured into the stromal bed of the recipient by using 16 interrupted 10–0 nylon sutures. Tobramycin-dexamethasone eye drops and ointment were used once daily for 14 days after lamellar keratoplasty. Follow-up

clinical examinations, including sodium fluorescein staining to assess epithelial integrity, slit-lamp to assess corneal optical clarity, neovascularization and degradation analyses of the grafts, and corneal topography analysis to assess corneal deformation, were conducted at 1, 3, 6, and 12 months postoperation, three rabbits were euthanized, and corneal specimens were prepared for H&E staining ($n = 3$).

2.11 | In vivo confocal microscopy examination

In vivo confocal microscopy images were obtained using a Heidelberg Retina Tomograph III Rostock Corneal Module (HRT III RCM, Heidelberg Engineering GmbH, Dossenheim, Germany) at 90 and 180 days postoperation. A drop of carbomer gel (Vidisic; Bausch & Lomb, Rochester, NY) was applied as the coupling medium between the applanating lens and the cornea. In vivo confocal microscopy of the central corneal graft was performed on each eye. At least 10 non-overlapping images were obtained for each area of the corneal epithelium. All rabbits were examined under general anesthesia.

2.12 | Statistical analysis

The values are presented as the mean \pm SD. Student's *t* test was used for statistical analysis to compare differences between the groups. A *p* value of $p < .05$ was considered statistically significant.

3 | RESULTS

3.1 | Decellularization efficiency

We compared the structures and components of DLPCS and NLPCS. Macroscopic images of DLPCS showed the same high degree of transparency as NLPCS (Figure 1a,b), corneal stromal nucleus scattered in stromal (Figure 1c), while there was no visible cellular debris in the H&E-stained DLPCS (Figure 1d). TEM showed that the lamellae of collagen fibrils in DLPCS maintained the same structure as NLPCS with slight cellular debris. The dry weight of DLPCS was 13.14 ± 1.78 mg, which was similar to the weight of NLPCS at 15.96 ± 1.83 mg ($n = 5$, $p > .05$). No cell membranes or cell organelles were observed, but a small amount of nucleic acid debris was observed in the corneal stroma compared with NLPCS (Figure 2a), as indicated by TEM (Figure 2b). The amounts of NLPCS and DLPCS DNA were 367.13 ± 19.96 and 15.41 ± 0.65 ng/mg in dry weight, respectively (Figure 2e, $n = 5$, $p < .05$).

3.2 | Ultrastructure of the stromal component

The collagen fibril lamellar arrangement and fibril ultrastructure of DLPCS was not notably different from those of NLPCS (Figure 2c,d). The collagen fibril diameter of DLPCS (27.06 ± 1.63 nm) was similar to that of NLPCS (26.58 ± 1.02 nm, $n = 5$, $p > .05$), and the collagen fibril spacing of DLPCS (25.61 ± 1.63 nm) was similar to that of NLPCS (26.39 ± 1.03 nm, $n = 5$, $p > .05$). There was no significant decrease in the collagen fibril spacing after the decellularization process ($n = 5$, $p > .05$).

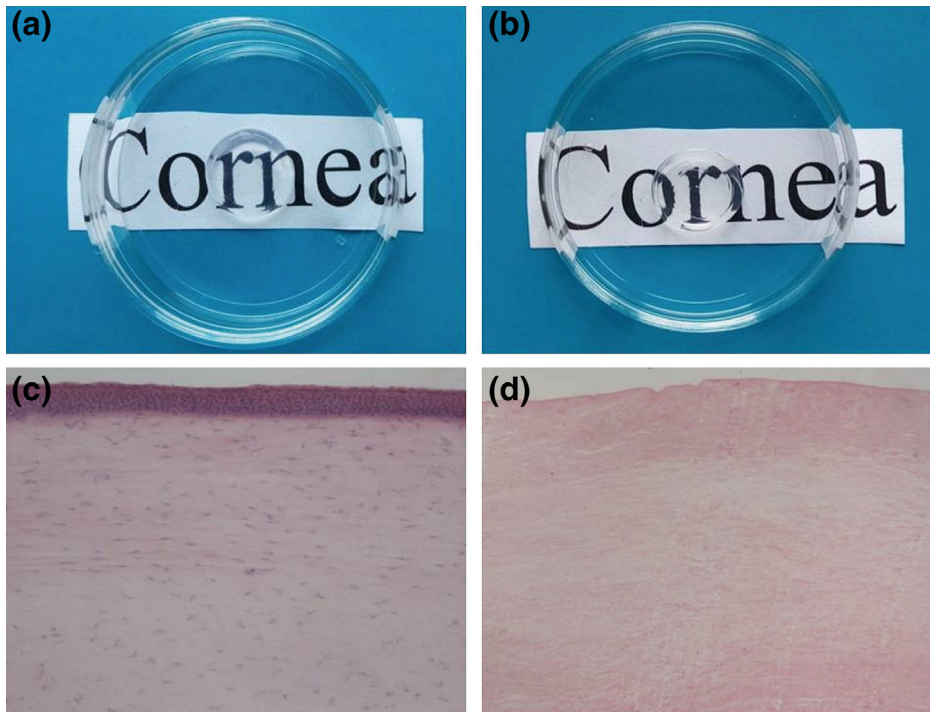
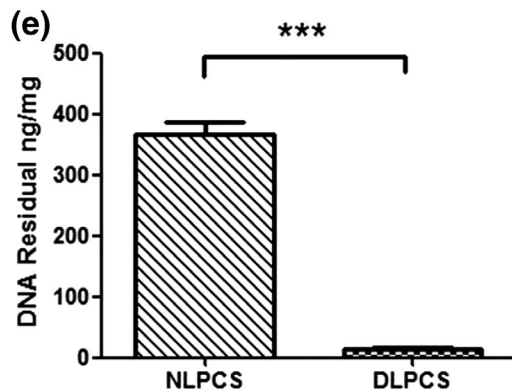


FIGURE 1 Decellularization efficiency with application of benzonase. (a) Macroscopic images of NLPCS. (b) DLPCS exhibited high transparency as NLPCS. (c) NLPCS in H&E staining. (d) DLPCS showed no sign of intact cell or cellular nuclear debris in H&E staining. (e) The amount of residual DNA in NLPCS and DLPCS



3.3 | Biocompatibility

As we used benzonase for decellularization, we analyzed the level of residual benzonase in the corneas and examined its potential toxic effects on cell proliferation and animal corneas. The residual benzonase level was less than the detection limit. The cell viability results demonstrated no significant differences in cell proliferation of the human corneal epithelial line, L-149 cell line and Vero cell line between the experimental and control groups ($n = 3$, $p > .05$). Toxicity was analyzed by directly injecting 0.1 ng benzonase into rabbit corneal stroma, and no corneal melting or neovascularization was observed, and corneal stromal edema gradually disappeared in 1 week ($n = 3$).

3.4 | Light transmittance

The light transmittance of DLPCS was not significantly different than that of NLPCS in the wavelength range of 380–780 nm (Figure 2f, $n = 3$).

3.5 | Lamellar keratoplasty in rabbits

We applied the prepared DLPCS that was treated with benzonase in rabbit corneas. All animals survived following implantation without infectious or hemorrhagic complications (Figure 3). The re-epithelialization started in 3 days postoperative (Figure 3a,b), one third plants repaired in 3 days postoperative (Figure 3c,d), completed at the time of 7 ± 2 days postoperative ($n = 12$, Figure 3e–h). The time to achieve sufficient transparency to clearly observe the iris for the DLPCS grafts was 24 ± 5 days ($n = 12$, Figure 3i). Corneal neovascularization, graft degradation, and corneal rejection were not observed at 12 months after transplantation. H&E staining showed that slight edema of the corneal stroma was observed at 1 month postoperation (Figure 3m), and the corneal stroma decreased gradually to a normal thickness (Figure 3n–p) without activated cells notably infiltrating the stroma during the entire observation period (Figure 3j–l).

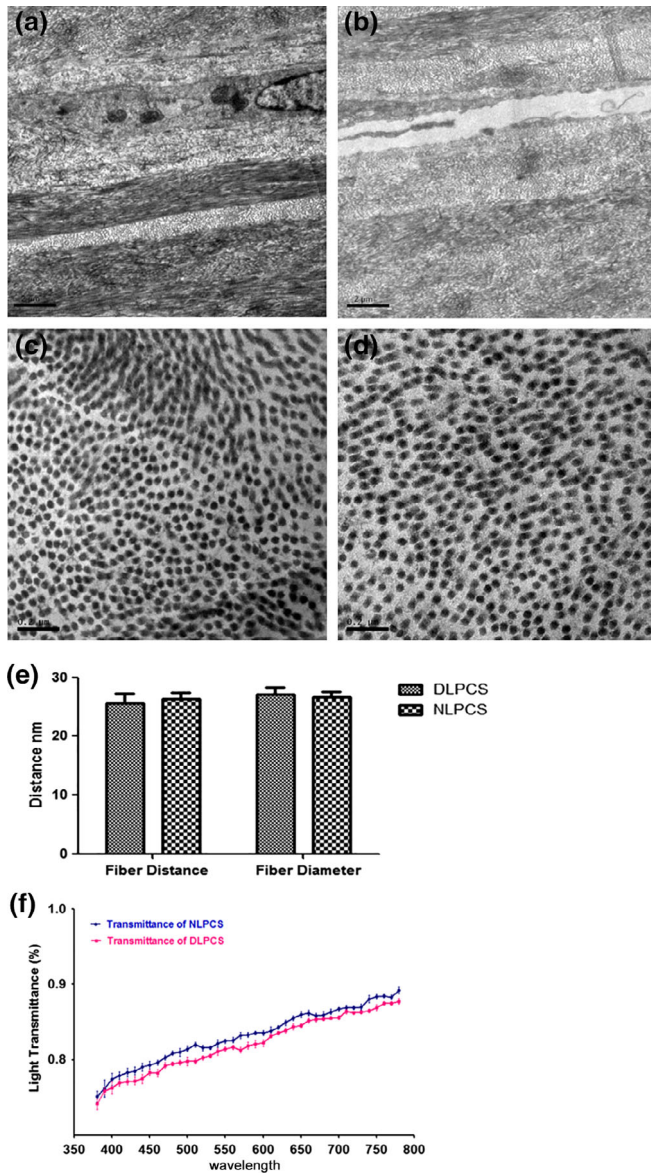


FIGURE 2 Representative images of TEM showed the collagen fibril arrangement in NLPCS and DLPCS. (a) Intact nucleus in NLPCS. (b) Similar collagen fibril arrangement in DLPCS with obvious spaces in the location of stromal cell with little cellular debris between collagen fibril lamella. (c and d) distances and diameters of collagen fibrils show in NLPCS (c) and DLPCS (d). (e) There was no statistical significant difference between these two groups. Light transmittance of the NLPCS and ALPCS over the wavelength range of 380–780 nm (f)

3.6 | In vivo confocal microscopy

We also examined and analyzed the transplanted corneas with in vivo confocal microscopy. The smooth surface of the corneal epithelium in the normal rabbit cornea was observed as a nearly 50-nm-depth with highly reflective cytoplasm and highly reflective nuclei (Figure 4a), while the surface epithelium in DLPCSs group was not sufficiently smooth (Figure 4e,i). It showed that there were large dark spaces which indicated the absence of epithelial cells, and these spaces gradually

decreased at 12 months postoperation in vivo confocal microscopy (Figure 4m). In the first month postoperation, the boundary of basal epithelial cells was undefined, and the reflectivity gradually increased (Figure 4n). The stromal nerve was much thinner than the normal nerve at 3 months and 6 months postoperation (Figure 4g,k), and the stromal nerve grew to a normal thickness after 12 months (Figure 4o). Furthermore, compared with the normal rabbit corneal basal epithelial density, which was 3789 ± 136 cells/mm² ($n = 3$, Figure 4b), the density of basal epithelial cells was 2871 ± 114 cells/mm² at 3 months postoperation ($n = 3$, Figure 4f), 2983 ± 128 cells/mm² at 6 months postoperation ($n = 3$, Figure 4j), and 3476 ± 145 cells/mm² at 12 months postoperation ($n = 3$, Figure 4n). Stromal cells were not observed after 1 month. Compared with the normal rabbit corneal basal epithelial density, which was 487 ± 69 cells/mm² ($n = 3$, Figure 4c), the density of stromal cells in the anterior stroma was 8 ± 21 cells/mm² after 3 months ($n = 3$, Figure 4g), 334 ± 65 cells/mm² after 6 months ($n = 3$, Figure 4k), and 389 ± 72 cells/mm² after 12 months ($n = 3$, Figure 4o). Furthermore, the nerve in the anterior stromal lamella was observed after 3 months. Corneal epithelial leukocytes were not observed in the normal control rabbits or rabbits that underwent lamellar keratoplasty. It was also revealed that the density and shape of corneal endothelial cells in the DLPCS-transplanted groups were similar to normal rabbit corneal endothelium (Figure 4d,h,i,p).

4 | DISCUSSION

The goal of our decellularization method was to efficiently remove xenogeneic nucleotides and proteins while minimizing adverse effects on collagen fibrils and the optical transparency of the corneal stroma. Therefore, we used the endonuclease benzonase, which efficiently degrades all forms of DNA and RNA without proteolytic activity in a wide range of conditions (pH values of 7.0–9.0 and temperatures of 15–55°C) (Wen, Xiao, Wang, & Wang, 2016; Ye et al., 2011). This endonuclease is a dimer consisting of 30 kDa subunits and is hydrophilic. The low molecular weight of benzonase makes it quickly infiltrate into corneal stroma, and it is easily removed by repeated washes. Chemical agents, such as alkaline and acidic substances, mechanical forces and high temperatures can easily cause corneas to lose transparency, which is typically seen in corneal traumas (Cellular and extracellular matrix modulation of corneal stromal opacity et al., 2014). But these factors are also often used in decellularization, which disturb the normal conformation of proteins and the regular arrangement of collagen fibrils. To provide optimal conditions for benzonase to efficiently degrade nucleotides with minimal loss of optical transparency due to ultrastructural damage, which can also be caused by lysosomes and proteases from ruptured stromal cells, we used bicarbonate-mixed salt solution (pH 7.5 and 20°C). In preliminary studies, we observed that the quantity of degraded DNA was positively correlated with the amount of benzonase and the time of operation under the same conditions. According to the time course curve of benzonase, we selected 5 hr as the termination timepoint, and benzonase removed over 99.5% of total DNA content. Residual

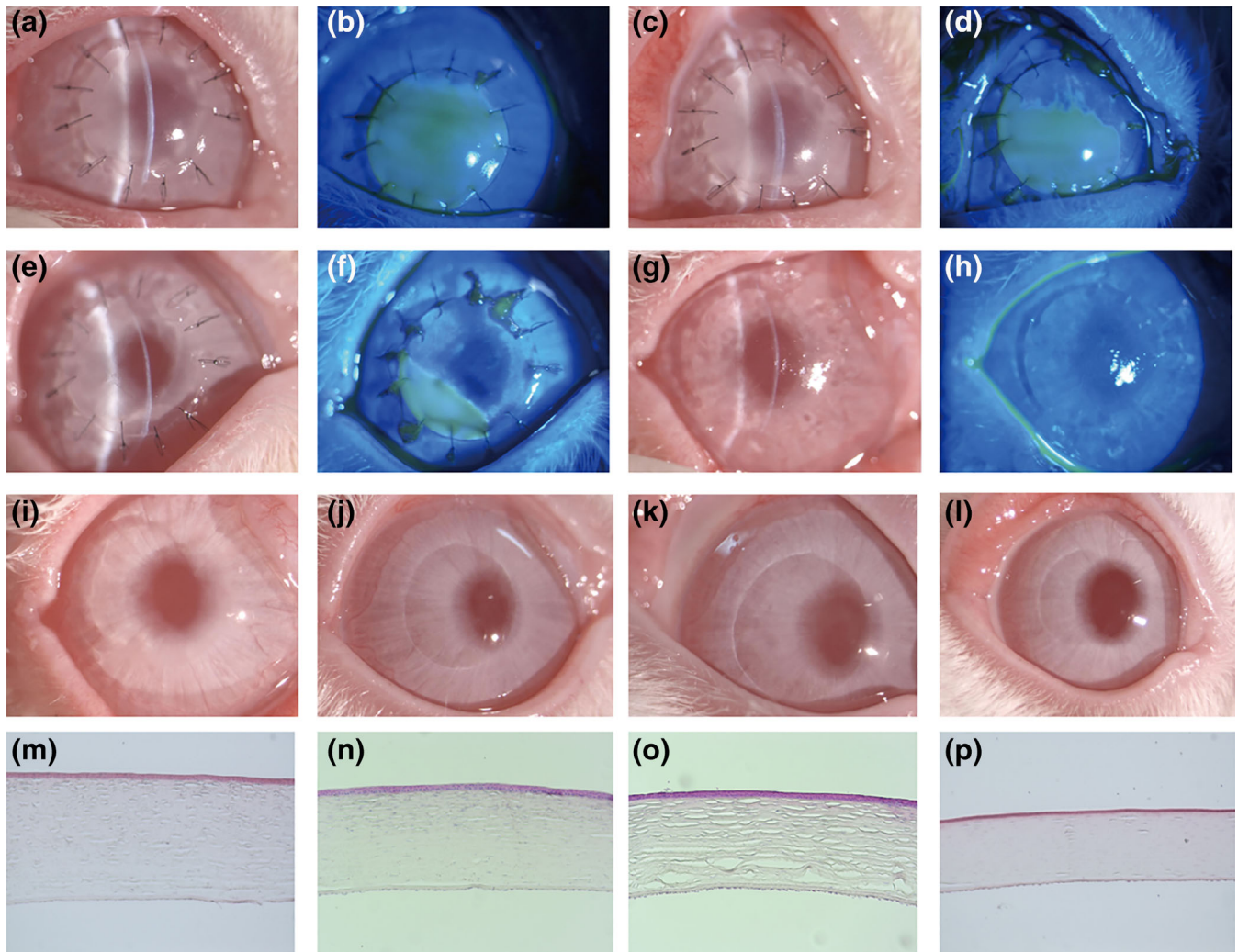


FIGURE 3 Postoperation observation of LKP with DLPCS. Three days postoperative, mild corneal edema (a) and corneal fluorescein staining showed a small amount of epithelia on the upper plate (b). Five days postoperative, corneal epithelium repaired over one third of plants surface with mild edema (c and d). One week postoperative, corneal edema decreased with over half of corneal epithelium repaired (e and f). Two weeks postoperative, corneal edema disappeared with whole epithelium repaired (g and h). The cornea restored to transparency after 1 month (i). The cornea kept transparency after 3 months (j). The cornea still showed transparency after 6 and 12 months, respectively (k and l). The representative images of corneal section in H&E staining of 1, 3, 6, and 12 months postoperative (m–p)

benzonase reached a low concentration after three washes because the endonuclease is water-soluble. To further determine whether enzymatic residues cause a corneal immune response, 0.1 ng benzonase was directly injected into normal rabbit corneal stroma. The cornea became transparent at 2 weeks postinjection, suggesting that the residual benzonase did not cause an immune response. Cell viability analysis demonstrated that DLPCS extracts were not cytotoxic in human corneal epithelial cells. The cytotoxicity of a high concentration of DLPCS in leaching liquor (1 piece of DLPCS in 1 mL of leaching liquor) was very low in HCECs, indicating that residual benzonase and cellular components do not affect HCEC proliferation.

The corneal epithelial basement membrane is important for epithelialization, which plays a crucial role in the maintenance of corneal stromal transparency in penetrating keratoplasty and lamellar keratoplasty (Cellular and extracellular matrix modulation of corneal stromal

opacity et al., 2014). Therefore, we kept Bowman's membrane and found that corneal epithelialization occurred in 1 week, which was as quick as human cornea transplantation. A regular arrangement of collagen fibrils was observed in normal clear corneal stroma, while collagen fibrils were not regularly arranged and disorganized in opaque corneal stroma (Piao, Zhou, Wu, & Chu, 2012; Wei et al., 2016). The regularity of collagen fibrils was assessed by distances between collagen fibers and the diameter of fibers using TEM. Except for the absence of nuclei, the TEM images showed that there were no obvious changes in the diameter, spacing, density, and border of collagen fibrils between the DLPCS and NLPCS groups, which were consistent with previous studies (Matteini, Rossi, Menabuoni, & Pini, 2007). After all preparation procedures, the transparency of DLPCS was the same as NLPCS in terms of general illumination and light transmittance, which was also indicated by clear and continuous blood vessels

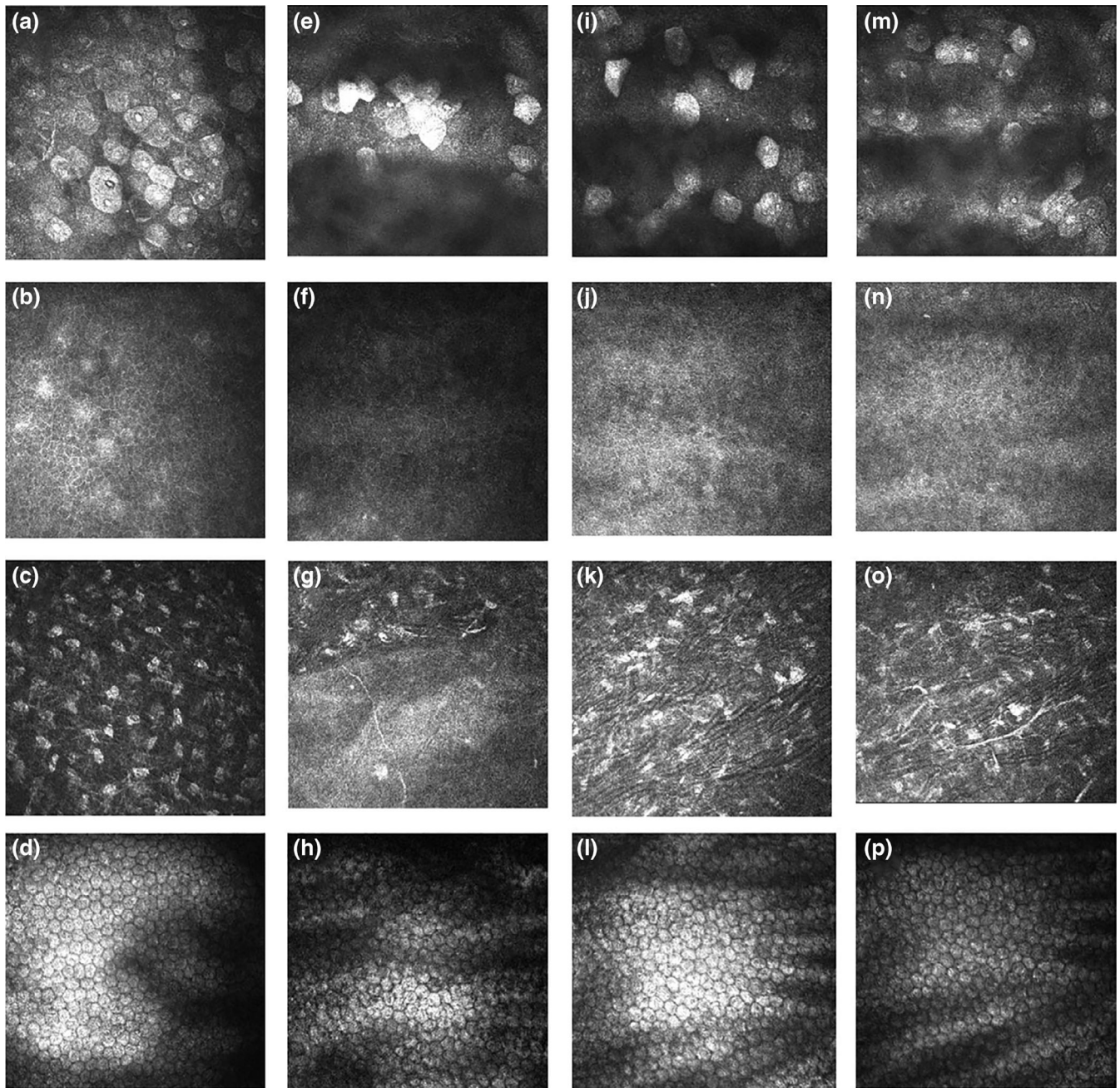


FIGURE 4 In vivo confocal microscopy examination and analysis of LKP in rabbit lamellar keratoplasty model. (a–d) Superficial corneal epithelium, basal corneal epithelium, anterior stroma, and endothelium in normal rabbit. (e–h) Superficial corneal epithelium, basal corneal epithelium, anterior stroma, and endothelium 3 months postoperation. (i–l) Superficial corneal epithelium, basal corneal epithelium, anterior stroma, and endothelium 6 months postoperation. (m–p) Superficial corneal epithelium, basal corneal epithelium, anterior stroma, and endothelium 12 months postoperation

behind the transparent cornea from the DLPCS graft in the central zone to the peripheral area of the cornea at 1 week postoperation. The corneal stroma continually remained transparent before and after re-epithelization.

Residual ionic and/or nonionic detergents used in decellularization processes have obvious cytotoxic effects, which result in inflammatory cells infiltration and corneal melting after lamellar keratoplasty (Crapo, Gilbert, & Badylak, 2011). The viability of human epithelial cells, Vero cells, and M149 cells indicated that benzoylase was not

cytotoxic and did not inhibit the proliferation of these cell lines. Subcutaneous pockets and lamellar keratoplasty showed very good tissue compatibility and the absence of infiltrated neutrophilic leukocytes and leukomonocytes.

In vivo confocal microscopy has become an increasingly popular noninvasive tool to examine the cornea at the cellular level and to better understand corneal cells and nerves. In this study, we used in vivo confocal microscopy to investigate changes in the cornea after lamellar keratoplasty in rabbit corneas. Superficial epithelial cells were

less smooth than normal corneal cells, showing a dark shade between cells at 1 month after surgery, and the cells gradually became smoother after half of a year, which was consistent with the H&E staining results. The density of basal epithelial cells recovered to a normal level, and the stromal cells grew back to cornea, while their density was less than that of normal corneal stromal cells. Several nerves in the anterior stroma were thinner than normal corneal anterior stromal nerves.

Corneal calcification, opacity, edema, and neovascularization are indications of rejection and constitute transplant failure (Kamp et al., 1995). Corneal transparency requires the following conditions for lamellar transplantation: intact epithelium, normal endothelial function, and regular arrangement of collagen fibers. The regular arrangement of corneal collagen fibers is the core of keeping acellular corneal stroma transparency after implantation. Regular arrangement of collagen fibers makes corneal stromal cells arrange regularly in the repair process. Collagen fibers secreted by corneal stromal cells reconstruct corneal ECM and keep cornea transparent. In this study, acellular corneal stroma obtained by benzonase is transparent after implantation, the transparency is enhanced after epithelialization, and the corneal stroma is always transparent after corneal reconstruction. In subcutaneous pockets and lamellar corneal transplants, none of the abovementioned indicators were observed in these animals within 12 months. Because of the high decellularization efficiency, no infiltration of neutrophilic leukocytes or leukomonocytes was observed after subcutaneous implantation of DLPCS. After decellularization, collagens and lamellar structures were not destroyed, and collagen fibril spacing remained too similar to that of the native stroma. Accordingly, the prepared DLPCS was highly transparent. A suitable scaffold material for corneal tissue engineering must simultaneously meet the challenges of biocompatibility, biomechanics and transparency for corneal transplantation. After lamellar keratoplasty, rabbit epithelial cells became flattened and elongated and migrated as an intact sheet to cover the whole DLPCS graft within approximately 7 days. The most common cause of corneal graft failure is irreversible immunological rejection with corneal neovascularization or ocular inflammation. During the course of graft epithelialization and transparency, there was no sign of infiltration of neutrophilic leukocytes or leukomonocytes. Within 12 months after lamellar keratoplasty, corneal neovascularization and haze were not observed.

5 | CONCLUSION

Decellularization is double-edged. An excessive procedure could cause permanent opacity of stromal tissue or a slow regaining of corneal transparency after transplantation. To explore the feasibility of decellularized corneas, we used benzonase to remove cellular components while minimizing the destruction of the ECM. The animal transplantation results also suggest that the decellularization of stromal cells with benzonase is an efficient and safe method.

ACKNOWLEDGMENTS

This work was supported by National Key R&D program of China (2018YFA0107304). Z. Liu is a recipient of Chinese Yangtze River Award.

ORCID

Zuguo Liu  <https://orcid.org/0000-0002-1737-5736>

REFERENCES

- Akanda, Z. Z., Naeem, A., Russell, E., J1, B., Si, F. F., & Hodge, W. G. (2015). Graft rejection and graft failure rate of penetrating keratoplasty (PKP) vs lamellar procedure: A systematic review. *PLoS One*, *17* (10), e0119934.
- Bertasi, G1., Cole, W2., Samsell, B3., Qin, X3., & Moore, M3. (2017). Biological incorporation of human acellular dermal matrix used in Achilles tendon repair. *Cell and Tissue Banking*, *18*, 403–411.
- Bueno, J. M., Gualda, E. J., & Artal, P. (2011). Analysis of corneal stroma organization with wavefront optimized nonlinear microscopy. *Cornea*, *30*, 692–701.
- Crapo PM1, Gilbert TW, Badylak SF. An overview of tissue and whole organ decellularization processes. *Biomaterials* 2011; *32*: 3233–3243.
- Ekser, B., Ezzelarab, M., Hara, H., van der Windt, D. J., Wijkstrom, M., Bottino, R., ... Cooper, D. K. (2012). Clinical xenotransplantation: The next medical revolution. *Lancet*, *379*, 672–683.
- Fischer L. M., Wolff M. W., Reichl U. (2018). Purification of cell culture-derived influenza. A virus via continuous anion exchange chromatography on monoliths. *Vaccine*. *36*, 3153–3160.
- Hara, H., & Cooper, D. K. (2011). Xenotransplantation—The future of corneal transplantation. *Cornea*, *30*, 371–378.
- Kamp, M. T., Fink, N. E., Enger, C., Maguire, M. G., Stark, W. J., & Stulting, R. D. (1995). Patient-reported symptoms associated with graft reactions in high-risk patients in the collaborative corneal transplantation studies. Collaborative Corneal Transplantation Studies Research. *Cornea*, *14*, 43–48.
- Lai, T., & Tang, S. (2014). Cornea characterization using a combined multiphoton microscopy and optical coherence tomography system. *Biomedical Optics Express*, *5*, 1494–1511.
- Lee, A., Ni, M. Y., Luk, A. C., Lau, J. K., Lam, K. S., Li, T. K., ... Wong, V. W. (2017). Trends and determinants of familial consent for corneal donation in Chinese. *Cornea*, *36*, 295–299.
- Matteini, P1., Rossi, F., Menabuoni, L., & Pini, R. (2007). Microscopic characterization of collagen modifications induced by low-temperature diode-laser welding of corneal tissue. *Lasers in Surgery and Medicine*, *39*, 597–604.
- Moore, M. A., Samsell, B., Wallis, G., Triplett, S., Chen, S., Jones, A. L., & Qin, X. (2015). Decellularization of human dermis using non-denaturing anionic detergent and endonuclease: a review. *Cell Tissue Bank*. *16*, 249–259.
- Moore MA1, Samsell B, Wallis G, Triplett S, Chen S, Jones AL, Qin X. Decellularization of human dermis using non-denaturing anionic detergent and endonuclease: A review. *Cell and Tissue Banking* 2015 Jun; *16*: 249–59.
- Piao MZ1, Zhou XT, Wu LC, Chu RY. Arg555Gln mutation of TGFBI gene in geographical-type Reis-Bücklers corneal dystrophy in a Chinese family. *The Journal of International Medical Research* 2012; *40*:1149–1155.
- Torricelli, A. A., & Wilson, S. E. (2014). Cellular and extracellular matrix modulation of corneal stromal opacity. *Exp Eye Res*. *129*, 151–160.
- Wei, S., Wang, Y., Wu, D., Zu, P., Zhang, H., & Su, X. (2016 Oct). Ultrastructural changes and corneal wound healing after SMILE and PRK procedures. *Current Eye Research*, *41*, 1316–1325.

- Wen, Y., Xiao, F., Wang, C., & Wang, Z. (2016). The impact of different methods of DNA extraction on microbial community measures of BALF samples based on metagenomic data. *American Journal of Translational Research*, 8, 1412–1425.
- Y1, Q., Wong, G., Monson, B., Stringham, J., & Ambati, B. K. (2010). Corneal transparency: Genesis, maintenance and dysfunction. *Brain Research Bulletin*, 81, 198–210.
- Ye, G. J., Scotti, M. M., Liu, J., Wang, L., Knop, D. R., & Veres, G. (2011). Clearance and characterization of residual HSV DNA in recombinant adeno-associated virus produced by an HSV complementation system. *Gene Therapy*, 18, 135–144.
- Zhang MC1, Liu X, Jin Y, Jiang DL, Wei XS, Xie HT. Lamellar keratoplasty treatment of fungal corneal ulcers with acellular porcine corneal stroma. *American Journal of Transplantation* 2015; 15:1068–1075.

How to cite this article: Liu J, Li Z, Li J, Liu Z. Application of benzonase in preparation of decellularized lamellar porcine corneal stroma for lamellar keratoplasty. *J Biomed Mater Res.* 2019;107:2547–2555. <https://doi.org/10.1002/jbm.a.36760>